ChemPubSoc Europe

DOI: 10.1002/cctc.201501232

CHEMCATCHEM Full Papers

Insights into the Major Reaction Pathways of Vapor-Phase Hydrodeoxygenation of *m*-Cresol on a Pt/HBeta Catalyst

Qianqian Sun,[a, b] Guanyi Chen,[b] Hua Wang,[a] Xiao Liu,[a] Jinyu Han,[a] Qingfeng Ge,*[a, c] and Xinli Zhu*[a, b]

Conversion of *m*-cresol was studied on a Pt/HBeta catalyst at 225–350 °C and ambient hydrogen pressure. At 250 °C, the reaction proceeds through two major reaction pathways: (1) direct deoxygenation to toluene (DDO path); (2) hydrogenation of *m*-cresol to methylcyclohexanone and methylcyclohexanol on Pt, followed by fast dehydration on Brønsted acid sites (BAS) to methylcyclohexene, which is either hydrogenated to methylcyclohexane on Pt or ring-contracted to dimethylcyclopentanes and ethylcyclopentane on BAS (HYD path). The initial hydrogenation is the rate-determining step of the HYD path as its rate is significantly lower than those of subsequent steps. The apparent activation energy of the DDO path is 49.7 kJ mol^{-1} but the activation energy is negative for the HYD path. Therefore, higher temperatures lead to the DDO path becoming the dominant path to toluene, whereas the HYD path, followed by fast equilibration to toluene, is less dominant, owing to the inhibition of the initial hydrogenation of *m*-cresol.

Introduction

Growing attention has been paid to the conversion of lignin, a major fraction of biomass, to valuable chemicals and fuels.[1–4] Depolymerization (such as fast pyrolysis) of lignin to phenolic compounds (phenol, guaiacol, syringol, and their derivatives[5,6]), followed by catalytic hydrodeoxygenation represents an important approach to reduce the oxygen content in fuel products from phenolics.[4,5]

In earlier work, studies of hydrodeoxygenation of phenolics were focused on using CoMoS and NiMoS catalysts at operating conditions similar to the industrial hydrodesulfurization processes (200–400 °C and high hydrogen pressures).[7–12] Two oxygenation removal pathways have been proposed based on the product distributions.[7,10] One produces aromatics by direct deoxygenation (the DDO path). The other produces cyclohexanes by saturating the phenyl ring, followed by deoxygenation (the HYD path).[7,10] This approach has the advantage of using commercially available technologies, but suffers from drawbacks including over hydrogenation and high cracking (and therefore high hydrogen consumption and low liquid fuel yields) owing to the severe operating conditions, fast catalyst deactivation owing to sulfur loss, as well as producing a sulfur-containing stream, which will burden the subsequent processes.

In the last decade, many studies have been performed by using nonsulfur catalysts under various conditions to develop an efficient deoxygenation process and to understand the reaction mechanisms.[4] Among these catalysts, transition metals supported on acidic supports, particularly zeolites, have been reported as efficient deoxygenation catalysts.[13–22] In liquid-phase reactions at low temperature and high pressure, it is generally accepted that hydrodeoxygenation of phenolics follows the HYD reaction path: the metal sites catalyze the hydrogenation of phenols to cyclohexanols, and then the zeolite acid sites catalyze the subsequent dehydration of cyclohexanols to cyclohexenes, which are finally hydrogenated to cyclohexanes on the metal sites.[13,14] By contrast, aromatics were found to be the predominant products for hydrodeoxygenation of phenolics on similar catalysts at relatively higher temperatures and lower pressures.[5,15,23–25] However, it is not yet clear whether the difference in product distributions originates from different reaction pathways, or from the same pathway but are shifted owing to the thermodynamic equilibrium between cyclohexanes and aromatics, the initial products of the reaction, as a result of the change in reaction conditions. Owing to the delocalization effect of the orbital containing the lone pair electrons of oxygen mixing with the π bond orbitals of the phenyl ring, the $C_{aromatic}$—OH is strengthened, resulting in a bond dissociation energy 84 kJ mol^{-1} higher than that of the $C_{aliphatic}$—OH bond in aliphatic alcohol.[26] Therefore, the direct deoxygenation path may be less favorable compared with the HYD path, in which the relatively weak $C_{aliphatic}$—OH bond can

[a] Q. Sun, Dr. H. Wang, Dr. X. Liu, Prof. J. Han, Prof. Q. Ge, Dr. X. Zhu
Collaborative Innovation Center of Chemical Science and Engineering
School of Chemical Engineering and Technology
Tianjin University
Tianjin 300072 (P.R. China)
E-mail: xinlizhu@tju.edu.cn

[b] Q. Sun, Prof. G. Chen, Dr. X. Zhu
School of Environmental Science and Engineering
State Key Laboratory of Engines
Tianjin University
Tianjin 300072 (P.R. China)

[c] Prof. Q. Ge
Department of Chemistry and Biochemistry
Southern Illinois University
Carbondale, Illinois 62901 (United States)
E-mail: qge@chem.siu.edu

easily break and eliminate water by a dehydration reaction on the acid sites of the zeolite. Additionally, the aromatics may be formed by subsequent fast dehydrogenation of cyclohexenes, which is thermodynamically favored at high temperatures. Indeed, a recent study reported that at 2 MPa and 300 °C, the hydrodeoxygenation of 4-propylphenol on Pt-Re/ZrO_2 catalyst follows the HYD path: hydrogenation to 4-propylcyclohexanol, followed by dehydration to 4-propylcyclohexene, and then dehydrogenation to propylbenzene as the final major product.[27]

The purpose of this work is to gain insights into the reaction pathways of the hydrodeoxygenation of phenolics over a Pt/HBeta catalyst. The reaction was carried out in the vapor phase and in the temperature range 225–350 °C to bridge the gap of the different results in the literature between low-temperature and high-pressure reactions and high-temperature and low-pressure reactions. *m*-Cresol (3-methylphenol) was selected as a simple model compound because (1) it is in liquid form at room temperature, which could be easily fed into the continuous-flow reaction system without using any solvent; (2) it is a major product from hydrodeoxygenation of guaiacol,[28–30] which is the most abundant component in bio-oil; and (3) the methyl group donates electrons to the phenyl π bond, and thus further strengthens the $C_{aromatic}$—OH bond,[24,31] making cresol deoxygenation the most difficult step in the deoxygenation of complex phenolics.

Results

Catalyst characterization

The XRD pattern of the reduced Pt/HBeta sample (data not shown) showed a BEA framework structure without any diffraction peaks belonging to Pt, indicating that Pt was highly dispersed on the HBeta support. Figure 1 shows a representative TEM image of the reduced sample. Pt particles of <4 nm uniformly distribute on the zeolite crystal, with a number-weighted average particle size of 1.7 nm. Some Pt particles with sizes smaller than 1 nm might reside in the micropores of HBeta. CO chemisorption studies estimate the Pt dispersion to be 0.77, giving an estimated Pt particle size of 1.3 nm. The difference in the Pt particle sizes estimated from TEM and CO chemisorption may be a result of a large fraction of Pt clusters or even single Pt atoms being located inside the micropores of zeolite, which cannot be easily observed in TEM, but are accessible to CO in the chemisorption study.

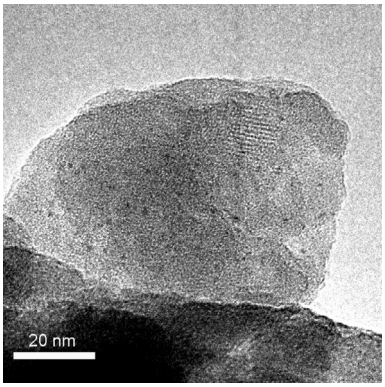

Figure 1. TEM image of reduced Pt/HBeta catalyst.

The acidity properties of Pt/HBeta are important as they may influence the reaction pathways. The NH_3 temperature-programmed desorption (TPD) profile (Figure 2 A) of the bare HBeta displays two desorption peaks at 205 and 345 °C, which are typically assigned to NH_3 desorption from weak acid sites and strong acid sites, respectively. Introducing 1% Pt to the HBeta resulted in the NH_3 desorption peaks shifting to lower temperatures with slightly reduced intensities. The quantified total acid densities are 0.723 and 0.695 mmol g^{-1} for HBeta and Pt/HBeta, respectively. Isopropylamine (IPA)-TPD was used to explore the Brønsted acidic properties of Pt/HBeta. Only the Brønsted acid sites (BAS) can catalyze the decomposition of IPA to propylene and ammonia, although Lewis acid sites may exist, but do not play a role.[32,33] Figure 2 B shows the $m/z=41$ profiles during IPA-TPD. The weak and broad peak at temperatures lower than 300 °C is generated from a fragment of IPA,

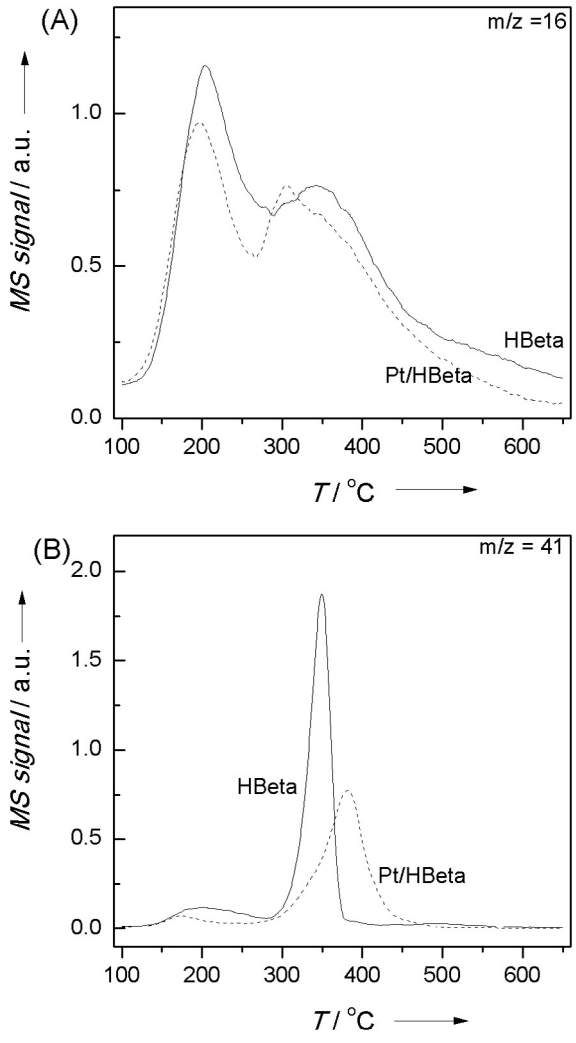

Figure 2. (A) NH_3-TPD and (B) IPA-TPD profiles of HBeta and Pt/HBeta catalysts.

whereas the strong peak at temperatures higher than 300 °C is due to propylene formed from the decomposition of IPA on BAS. The propylene peak centered at 350 °C is sharp for HBeta, whereas it is shifted to the higher temperature of 383 °C on Pt/HBeta with a broadened peak, indicating that the acid strength was weakened as a result of Pt loading. The measured BAS densities are 0.695 and 0.674 mmol g^{-1} for HBeta and Pt/HBeta, respectively. The measured BAS density from IPA-TPD is slightly lower than the total acid density from NH_3-TPD, which implies that the major acid sites are Brønsted type. Comparison between Pt/HBeta and bare HBeta suggests that at least parts of the Pt clusters are in close contact with the acid sites, and, therefore, reduce the number of accessible acid sites and weaken the acid strength owing to the interaction between the acid sites and Pt clusters. It should be noted that the molar ratio of BAS to surface Pt site is 17.

m-Cresol conversion at 350 °C

Figure 3 illustrates the evolution of major products as a function of space time (W/F)—defined as the ratio of catalyst mass to organic feed flow rate ($g_{cat}\ g_{reactant}^{-1}$ h)—at 350 °C. Clearly, toluene (Tol) is the major and primary product from hydrodeoxygenation of *m*-cresol. At low W/F, besides hydrodeoxygenation, the isomerization of *m*-cresol to *p*- and *o*-cresol isomers (Iso-Cr) and transalkylation of cresol isomers to phenol (Ph) and xylenol isomers (Xol) on BAS also appear to be important reactions. However, they eventually convert to Tol, benzene (Ben), and xylenes (Xyl) when W/F is increased to 0.4 h. The yields of methylcyclohexane (MCHane) and ring-contraction (RC) products are close to zero, and the possible intermediates of the HYD path are not observed. This product distribution suggests that DDO is the major reaction path (Figure 4), in agreement with the previously reported results at 400 °C.[5,24]

As also shown in Figure 4, the formation of toluene may follow the HYD path, constrained by the thermodynamic equilibration with Tol. To test this hypothesis, 3-methylcyclohexanol (MCHol), an important intermediate of the HYD path, was used as a reactant. As displayed in Figure 5, MCHol is quickly dehydrated to methylcyclohexene (MCHene) with an intrinsic reaction rate two orders of magnitude faster than that of hydrodeoxygenation of *m*-cresol. As W/F is increased, the MCHene formed initially converts to the RC products on BAS, or to MCHane and Tol on the Pt sites through hydrogenation/dehydrogenation reactions. The overall intrinsic reaction rate of MCHene conversion is one order of magnitude faster than that of hydrodeoxygenation of *m*-cresol. Note that Tol is the least favorable product from MCHene conversion at low W/F. Further increases in W/F lead to the RC products and MCHane converts further to the thermodynamically more favorable Tol through the ring enlargement and dehydrogenation reactions. When W/F is higher than 0.1 h, Tol becomes the dominant product. Importantly, at W/F = 0.5 h, MCHol produces the same Tol yield, of approximately 83 %, as that of the *m*-cresol feed (Figure 3). At first glance, one may argue that hydrodeoxygenation of *m*-cresol may also follow the HYD path with the intermediate products [3-methylcyclohexanone (MCHone), MCHol, MCHene] being quickly converted and, thus, not observable.

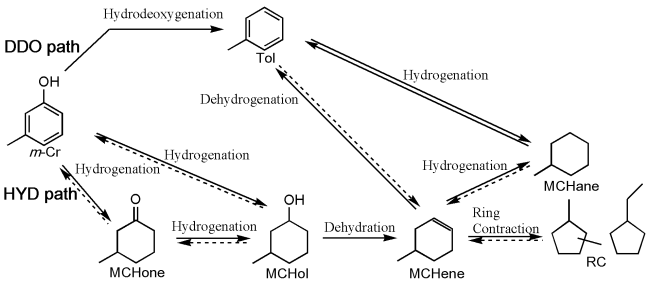

Figure 4. Major reaction path of *m*-cresol conversion on Pt/HBeta. Note that acid-catalyzed cresol isomerization and transalkylation are not included in this scheme.

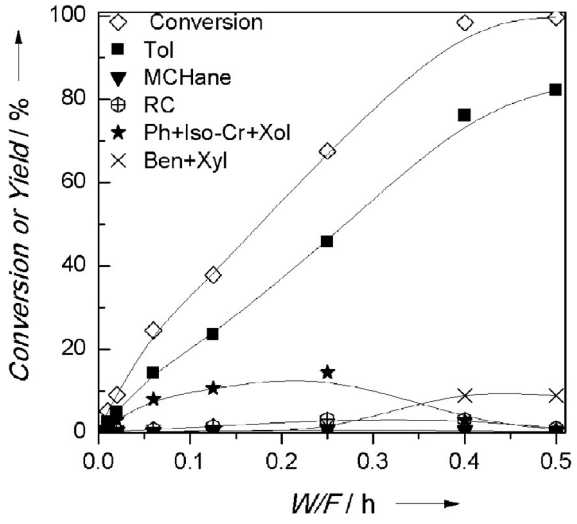

Figure 3. Effect of W/F on *m*-cresol conversion and major products distribution on Pt/HBeta at 350 °C. Reaction conditions: $T = 350$ °C, $P = 1$ atm, H_2/*m*-cresol = 50, Time on stream (TOS) = 0.5 h for each W/F.

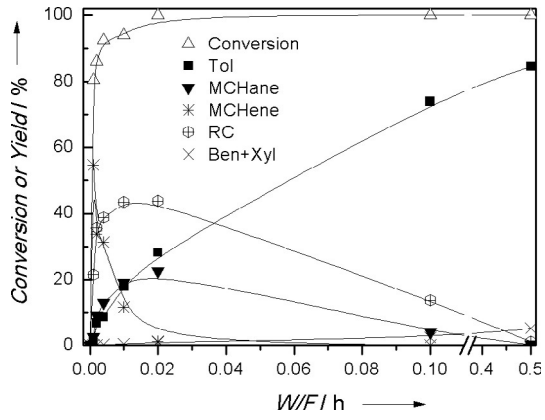

Figure 5. Effect of W/F on methylcyclohexanol (MCHol) conversion and major products distribution on Pt/HBeta at 350 °C. Reaction conditions: $T = 350$ °C, $P = 1$ atm, H_2/MCHol = 50, TOS = 0.5 h for each W/F.

m-Cresol conversion at 250 °C

To determine which reaction path the hydrodeoxygenation of *m*-cresol follows, we lowered the reaction temperature to 250 °C. At this temperature, the conversion of *m*-cresol increases almost linearly with W/F, and complete conversion requires a W/F of 1 h (Figure 6A). At low W/F (Figure 6A, inset), the yields of MCHone, MCHane, and Tol are almost the same, whereas the yield of the RC products is rather low. Increasing W/F leads to fast reduction of MCHone to almost zero and a significant increase in the RC products, making the latter one of the major products on the scale of MCHane and Tol (Figure 6B). Again, isomerization and transalkylation products (Ph + Iso-Cr + Xol) are observed at intermediate W/F values, with yields being lower than those at 350 °C. These intermediates are finally deoxygenated to Ben, Tol, and Xyl. This product evolution might suggest that the reaction follows the HYD path (Figure 4): *m*-cresol is first hydrogenated to MCHone and MCHol on Pt, MCHol is then quickly dehydrated on the adjacent BAS to MCHene, which either hydrogenates to MCHane or dehydrogenates to Tol on Pt with a faster rate than the ring contraction to form the RC products on BAS.

Further analysis of the distribution of RC products (Figure 6C) shows some interesting features. At low W/F, ethylcyclopentane (ECP) appears to be the major product. At high W/F, the yields of dimethylcyclopentane (DMCP) isomers increase quickly and replace ECP as the major products. The yields of the DMCP isomers follow the order of 1,3-DMCP > 1,2-DMCP > 1,1-DMCP.

Although Tol also appears to be one of the primary products at low W/F, the contribution to its formation from the HYD path, followed by fast equilibration from MCHene and MCHane to Tol, cannot be excluded. If Tol comes mainly from the HYD path, one would expect that the conversion of intermediate products of the HYD path could result in the same Tol yield at similar reaction conditions as that of *m*-cresol. Therefore, we tested all the possible intermediates to explore if Tol was mainly from the HYD path.

When MCHone is fed into the reaction (Figure 7) at low W/F, MCHene is the first to appear in a significant amount, followed by MCHane, whereas Tol, RC, and *m*-cresol (*m*-Cr) are almost zero. This result indicates that the primary and major reaction is hydrogenation of MCHone to MCHol as well as the subsequent fast dehydration to MCHene, followed by hydrogenation to MCHane. The low yields of Tol and RC products at low W/F indicate that dehydrogenation on Pt and ring contraction on BAS are less favorable than hydrogenation of MCHene to MCHane on Pt under the kinetic control regime of the current reaction conditions. The yields of RC and Tol increase slowly with increasing W/F, and they are less than 5% and 4%, respectively, at W/F of 1 h. It is important to note that the Tol yield of 4% is about eight times lower than that of 31% for *m*-cresol at W/F of 1 h (Figure 3). This test indicates that MCHone cannot produce Tol with a similarly high yield as *m*-cresol under the same reaction conditions. It should be noted that besides the hydrodeoxygenation-related reactions, other side reactions (such as aldol condensation[34,35]) catalyzed by the

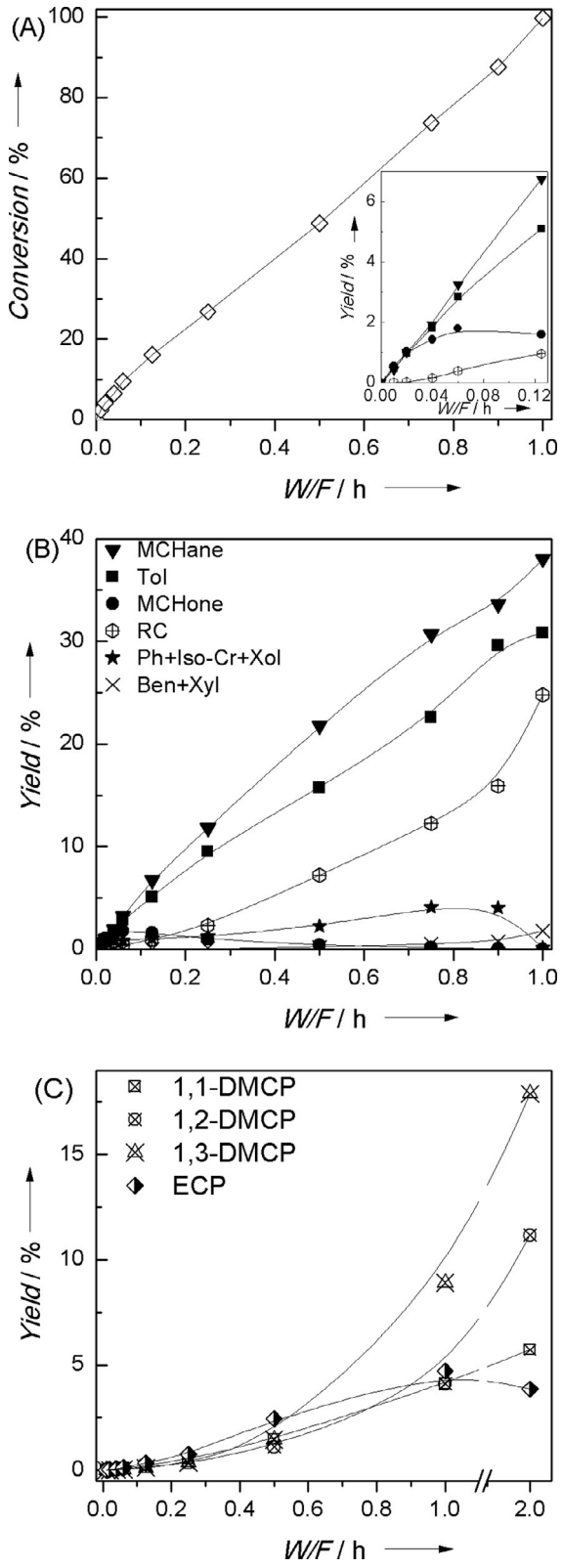

Figure 6. Effect of W/F on *m*-cresol conversion (A), major products distribution (B), and RC products distribution (C) on Pt/HBeta at 250 °C. Inset: major product yields at low W/F. Reaction conditions: $T = 250$ °C, $P = 1$ atm, H_2/*m*-cresol = 50, TOS = 0.5 h for each W/F.

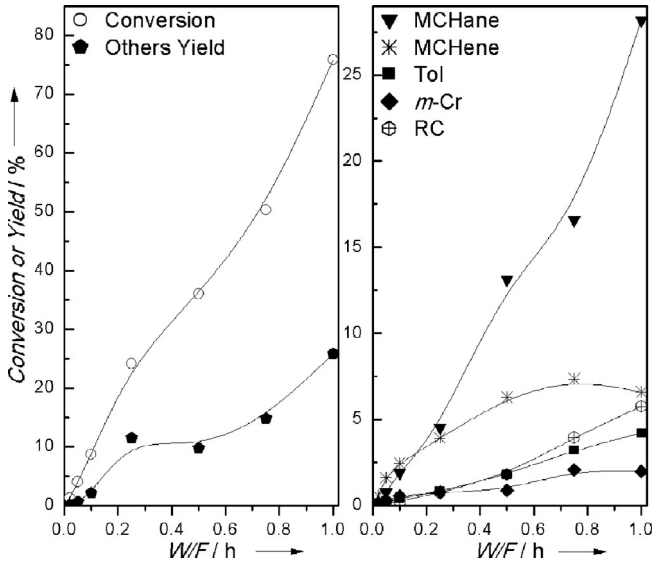

Figure 7. Effect of W/F on methylcyclohexanone (MCHone) conversion and major products distribution on Pt/HBeta at 250 °C. Reaction conditions: $T = 250$ °C, $P = 1$ atm, H_2/MCHone = 50, TOS = 0.5 h for each W/F.

bare acid sites can lead to a significant amount of other bicyclic products (Figure 7).

Figure 8 shows the product evolution as a function of W/F for the feed of MCHol. At very low W/F, MCHene is the only primary product from dehydration of MCHol on BAS. Increasing W/F results in the hydrogenation of MCHene to MCHane as the major path over that of ring contraction on BAS or dehydrogenation to Tol on Pt. At W/F = 0.02 h, MCHene is completely converted to MCHane (66%), RC products (21%), and Tol (9%). Note that the Tol yield is three times lower than that of 31% for *m*-cresol at W/F = 1 h, indicating that MCHol cannot produce a similar yield of Tol to the *m*-cresol feed. To confirm

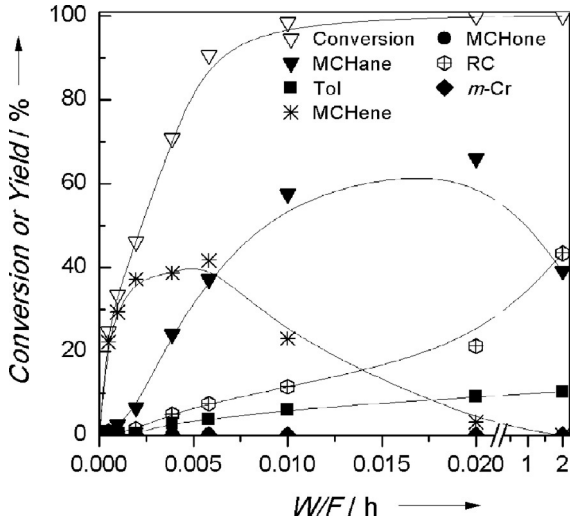

Figure 8. Effect of W/F on methylcyclohexanol (MCHol) conversion and major products distribution on Pt/HBeta at 250 °C. Reaction conditions: $T = 250$ °C, $P = 1$ atm, H_2/MCHol = 50, TOS = 0.5 h for each W/F.

this conclusion, we increased W/F to 2 h, but the yield of Tol remains at 9%.

To map out the major reaction pathways, MCHene, MCHane and Tol were fed into the reaction in turn. For the MCHene feed (Figure 9A), MCHane is the primary and major product, while RC products and Tol are minor products. The yield of MCHane is at least six times more than that of Tol. This further confirms that the hydrogenation of MCHene to MCHane on Pt is significantly faster than that of dehydrogenation to Tol on Pt or ring contraction to RC products on BAS, as was observed when MCHone and MCHol were used as the feeds. It should be noted that the isomerization of MCHene (double bond shift) is also notable but has been treated as unconverted MCHene (Figure 9A). For the MCHane feed (Figure 9B), the RC products and Tol are observed, with the ring contraction being more favorable over the dehydrogenation to Tol. When Tol is fed into the reaction (Figure 9C), hydrogenation of Tol to MCHane is more favorable than the ring contraction to the RC products at low W/F. When W/F is high, MCHane formed in the reaction converts further to the RC products. These results demonstrate that the interconversion of deoxygenated products of MCHane, MCHene, and Tol to the RC products on Pt/HBeta (Figure 4) complicates the reaction pathway.

It is interesting to note that MCHene was observed when the MCHone and MCHol were the feeds but not when the feeds were MCHane or Tol. This difference can be attributed to the different active sites for the formation of MCHene. For MCHone and MCHol, MCHene is formed through dehydration on BAS with high rates. High quantities of MCHene could (i) desorb to the gas phase; (ii) stay on the BAS for RC reaction with slower rates than dehydration; (iii) diffuse to the adjacent Pt sites for hydrogenation or dehydrogenation reactions. As for MCHane and Tol, the formation of MCHene occurs on the Pt sites. The hydrogenation/dehydrogenation are fast, without MCHene being released to the gas phase.[36] A small quantity of surface MCHene may diffuse to the adjacent BAS for the ring-contraction reaction.

As none of the major intermediates (MCHone, MCHol, MCHene) of the HYD path produce Tol with as high a yield as that of *m*-cresol at low W/F under kinetic control of the product distribution or at high W/F under thermodynamic control of the product distribution, we can conclude that two distinct reaction pathways exist for hydrodeoxygenation of *m*-cresol under the current reaction conditions. As shown in Figure 4, one reaction path is the direct deoxygenation of *m*-cresol to Tol (DDO path), the other is hydrogenation of *m*-cresol to MCHone and MCHol, dehydration to MCHene, followed by fast hydrogenation to MCHane on Pt or slow ring contraction to RC products on BAS (HYD path). The contribution of the HYD path to the formation of Tol is negligible at low W/F (or low conversion) and not important at high W/F (or high conversion).

Effect of reaction temperature on *m*-cresol conversion

It is apparent that the product distributions are significantly different at 250 °C and 350 °C. To explore how the reaction

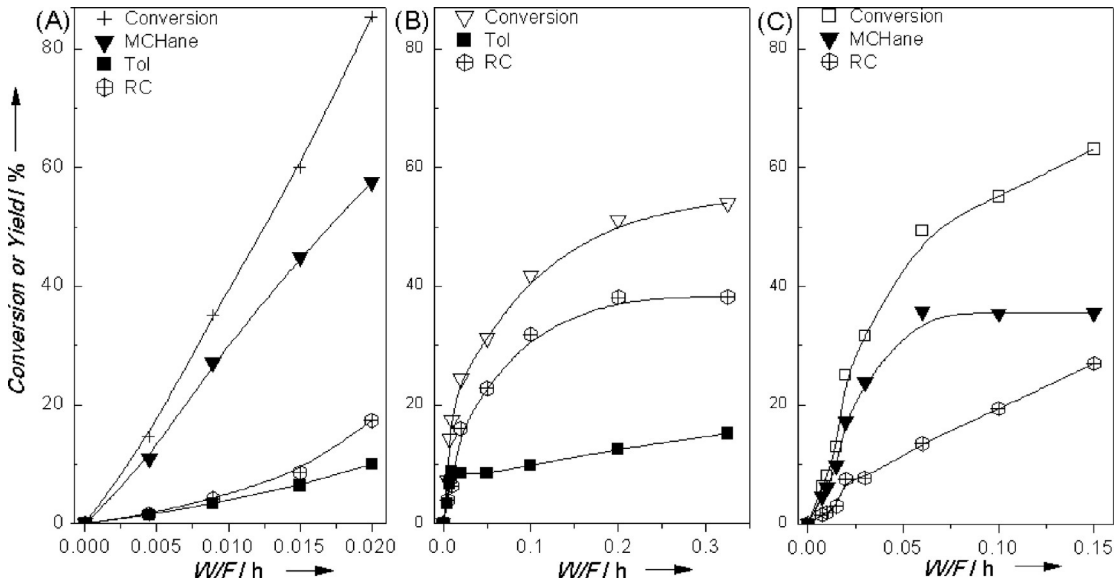

Figure 9. Effect of W/F on methylcyclohexene (A), methylcyclohexane (B), and toluene (C) conversion on Pt/HBeta at 250 °C. Reaction conditions: $T = 250$ °C, $P = 1$ atm, H_2/reactant = 50, TOS = 0.5 h for each W/F.

temperature affects the product distribution, we further investigated the conversion of *m*-cresol over the temperature range of 225–350 °C using a W/F of 0.5 h. Note that this range covers the broad reaction temperature range of studies of hydrodeoxygenation of phenolics in the literature. As shown in Figure 10, *m*-cresol conversion increases almost linearly from 32 to 99% with increasing temperature. MCHane and Tol are the dominant products at 225 °C. Increasing the temperature causes the Tol yield to increase monotonically, whereas the yield of MCHane gradually decreases to zero at 350 °C. The yield of the RC products increases to a maximum at 300 °C, and then decreases to zero. The yields of the isomerization and transalkylation products are lower than 5% over this temperature range. They are finally converted to Tol, Ben, and Xyl at 350 °C.

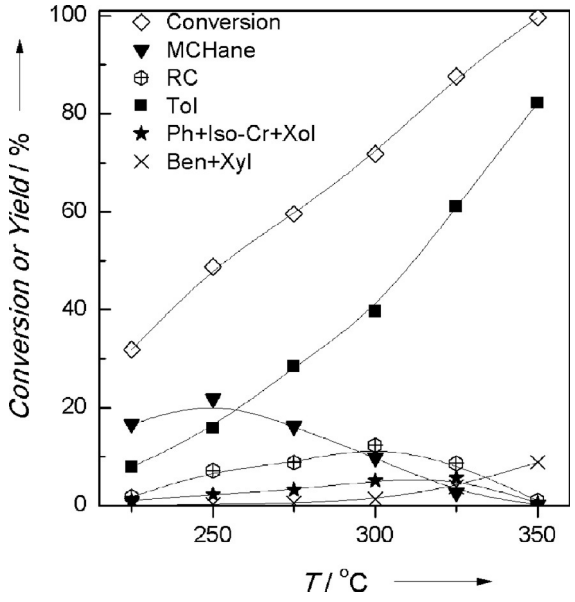

Figure 10. Effect of reaction temperature on *m*-cresol conversion on Pt/HBeta at a W/F value of 0.5 h. Reaction conditions: $P = 1$ atm, H_2/*m*-cresol = 50, TOS = 0.5 h, W/F = 0.5 h.

Discussion

Role of Brønsted acid sites on the reaction pathway of *m*-cresol at 250 °C

In previous work, it has been demonstrated that the major reaction pathways of *m*-cresol conversion on a Pt/SiO_2 catalyst at 250 °C and at atmospheric H_2 pressure are the direct hydrodeoxygenation to Tol and hydrogenation to MCHone and MCHol, with the hydrogenation rate faster than that of hydrodeoxygenation.[37] The HYD path stops at the hydrogenation step because of the lack of acidity on silica to catalyze the dehydration of MCHol and low C–O hydrogenolysis activity of MCHol on Ni, Pd, and Pt catalysts. The MCHone and MCHol originally formed have to be dehydrogenated back to *m*-cresol and then deoxygenated to Tol at high *m*-cresol conversions.[37] The reversible interconversion of *m*-cresol, MCHone, and MCHol through hydrogenation and dehydrogenation on bare metal catalysts has also been observed under similar reaction conditions.[25,38–40]

However, when Pt was supported on acidic HBeta, the HYD reaction path becomes accessible. In contrast to the Pt/SiO_2 catalyst, dehydrogenation of MCHone to *m*-cresol is negligible on Pt/HBeta (Figure 7). Similarly, dehydrogenation of MCHol to MCHone and *m*-cresol is absent on Pt/HBeta (Figure 8). These results indicate that the presence of acid sites on HBeta enabled the dehydration reaction with a significantly higher rate than that of the dehydrogenation reaction, making the hydrogenation products (MCHone and MCHol) almost irreversibly dehydrate to MCHene. Table 1 compares the intrinsic reaction rates and turnover frequencies (TOF) of the conversions of the

Table 1. Comparison of the reaction rates and turnover frequencies (TOF) for different feeds on Pt/HBeta at 250 °C.

	Feed					
	m-cresol	MCHone	MCHol	MCHene	MCHane	Tol
Rate[a] [μmol g_{cat}^{-1} s^{-1}]	4.87	1.93	1239	96	48	25
TOF_{Pt}[b] [s^{-1}]	0.10	0.04		2.05	1.22	0.64
TOF_{BAS}[c] [s^{-1}]	0.0014	0.0005	1.84	0.016		

[a] The reaction rate and TOF were measured at conversions less than 15%. [b] TOF of Pt-catalyzed reactions. [c] TOF of Brønsted acid site catalyzed reactions.

different feeds at 250 °C, measured at a conversion of less than 15%. The reactions initiated on Pt (direct deoxygenation and hydrogenation/dehydrogenation) account for the TOF_{Pt}, calculated in terms of the number of surface Pt atoms measured by CO chemisorption, and the reactions that took place on BAS account for the TOF_{BAS}, calculated on the basis of the IPA-TPD measured acid density. The acid-catalyzed reactions include: isomerization and transalkylation for *m*-cresol, condensation for MCHone, dehydration for MCHol, and ring contraction for MCHene. From Table 1, it is evident that the reaction rate of dehydration of MCHol is about 2–3 orders of magnitude higher than the other reactions. This high reaction rate can be attributed to both the high BAS density (i.e., high BAS/Pt ratio) and the high TOF of dehydration. Indeed, the TOF of MCHol dehydration is ~10 times higher than the hydrodeoxygenation and hydrogenation of *m*-cresol and MCHone. As a result, the MCHol formed is quickly consumed by dehydration, making it barely observable when *m*-cresol and MCHone were fed into the reaction (Figure 6 and 7). Therefore, one could expect that once MCHol is formed, the reaction of *m*-cresol would irreversibly proceed through the HYD path. In addition, the intrinsic reaction rate and TOF of MCHene conversion are ~20 times higher than those of *m*-cresol and MCHone (Table 1), which leads to a fast conversion of MCHene formed from dehydration to MCHane preferably at a low conversion. As a consequence of the significantly higher rates of MCHol dehydration and MCHene conversion, the formation and consumption of MCHol and MCHene reach a steady state and their yields are negligibly low in *m*-cresol conversion. The fast production of MCHane makes it appear to be one of the primary products, like Tol and MCHone, at low *m*-cresol conversions (Figure 6).

Owing to the fact that the dehydration of MCHol and hydrogenation of MCHene are significantly faster than the Pt-catalyzed hydrogenation of *m*-cresol, the rate-determining step for the HYD path is the initial hydrogenation of *m*-cresol to MCHol on Pt. Therefore, the selectivity of following the DDO and HYD path is dependent on the balance of the initial reactions between the direct deoxygenation to Tol and hydrogenation to MCHone and MCHol.

Effect of the reaction temperature on the reaction pathway of *m*-cresol

When the reaction temperature is increased to 350 °C, thermodynamic equilibrium drives the interconversion between the primary deoxygenation products (Tol, MCHene, MCHane, and RC) with significantly enhanced reaction rates, which may mask the true reaction pathway. Detailed analysis of the product distributions from MCHol (Figure 5) and *m*-cresol (Figure 3) may provide insights into the true reaction pathway. As compared in Table 2, at W/F = 0.02 h when MCHene formed from MCHol is almost completely converted to the final products (Figure 5), the yields of MCHane and RC are significantly higher than those observed for the *m*-cresol feed. In addition, at W/F = 0.1 h when the yield of MCHane is reduced to a low value for the MCHol feed (Figure 5), the yield of the RC products is still ~10 times higher than that for the feed of *m*-cresol at a similar W/F of 0.125 h. These differences in product distribution between the MCHol and *m*-cresol feeds at similar W/F values indicate that the reaction pathways of *m*-cresol and MCHol are different. Furthermore, when both feeds convert completely with the same yield of Tol at W/F = 0.5 h, the yields of Ben and Xyl from *m*-cresol are almost twice that from MCHol. This result provides further evidence that the *m*-cresol and MCHol deoxygenation reactions proceed through different pathways. For *m*-cresol, the transalkylation reaction happens readily as a primary reaction on BAS,[23,24] and the subsequent direct deoxygenation leads to the formation of Ben and Xyl with high yields. In contrast, the transalkylation reaction is not expected to occur for MCHols, but takes place for Tol. Tol is not a kinetically favored product from MCHene (see Figures 5, 8, and 9A). Its formation requires a high W/F value as a result of the thermodynamic equilibration from the MCHane and RC products (see Figure 5). This leads to lower yields of the tertiary products of Ben and Xyl from the secondary product of Tol. Thus, at 350 °C, the HYD path followed by fast thermodynamic equilibration to Tol is not important,

Table 2. Comparison of the product distribution of *m*-cresol and methylcyclohexanol conversion on Pt/HBeta at 350 °C and similar W/F values.

Feed	W/F [h]	Conversion [%]	Yield of major products [%]						
			Tol	MCHane	MCHene	RC	Iso-Cr + Ph + Xol	Ben + Xyl	Others[a]
m-cresol	0.02	5.2	2.56	0.07	0	0.14	2.2	0.02	0.2
	0.125	37.8	23.6	0.45	0	1.46	10.7	0.49	1.1
	0.5	100	82.2	0.19	0	1.07	0.07	9.0	7.8
MCHol	0.02	100	28.2	22.5	1.3	43.4	0	0.97	3.7
	0.1	100	74.0	4.06	0	13.7	0	2.4	5.8
	0.5	100	84.6	0.29	0	1.13	0	5.1	8.9

[a] Sum of other products.

whereas the DDO path to Tol is the predominant reaction path for *m*-cresol conversion.

As discussed previously, the rate-determining step for the HYD path is the initial hydrogenation of *m*-cresol. Even though the dehydration rate of MCHol is increased as the temperature is raised, the hydrogenation step would become less favorable as it is a strongly exothermic reaction,[25,26,40–42] resulting in a reduced contribution of the HYD pathway to the overall conversion. To verify this, MCHone, tautomer of the partial hydrogenation product of *m*-cresol, was tested. Compared with MCHone conversion at 250 °C (Figure 7), a significantly different product distribution is observed at 350 °C (Figure 11). Although the *m*-cresol and Tol yields are tiny at 250 °C, they become the major products when the reaction temperature is increased to 350 °C. If the yields of isomerization and transalkylation products (Iso-Cr + Ph + Xol) of *m*-cresol and their deoxygenation products (Ben + Xyl) are included, the yields of *m*-cresol and Tol and their secondary products are the dominant products in the conversion of MCHone at 350 °C. In contrast, MCHane and MCHene are the major products of MCHone conversion at 250 °C, but they become minor products at 350 °C. These results indicate that the dehydrogenation of MCHone to *m*-cresol followed by direct deoxygenation to Tol is more favorable than its hydrogenation to MCHol to proceed through the HYD path to MCHene, RC products, and MCHane. As MCHone, which has four hydrogen atoms added to the phenyl ring, can be easily dehydrogenated to *m*-cresol, one would expect that the surface intermediates with fewer carbon atoms being hydrogenated in the phenyl ring will be much easier to dehydrogenate and reproduce *m*-cresol than hydrogenation to MCHone and then to MCHol to proceed through the HYD path. Therefore, although the MCHol dehydration rate is enhanced, the hydrogenation of *m*-cresol to MCHol, that is, the rate-determining step of the HYD path, is significantly retarded, resulting in the HYD path not playing an important role for *m*-cresol conversion at 350 °C.

It is interesting and important to analyze the activation energies of the DDO and HYD paths for the hydrodeoxygenation of *m*-cresol on Pt/HBeta. As discussed above, Tol is the least favorable product, with negligible yield from MCHene following the HYD path in the kinetic control regime (Figure 9), Tol can therefore be approximately treated as a product exclusively from the DDO path at low *m*-cresol conversions. Similarly, the tiny amounts of Ben and Xyl can also be treated as the products from the direct deoxygenation of Ph and Xol. However, MCHone, MCHol, MCHene, MCHane, and the RC products are produced through the HYD path at low *m*-cresol conversions. Figure 12 shows the Arrhenius plots between 225–350 °C. The reaction rate was measured under a *m*-cresol conversion of less than 7% by adjusting W/F. It should be noted that the isomerization and transalkylation products were included with the unconverted *m*-cresol, as these reactions are catalyzed by BAS without the participation of Pt.[24] The plots yield an apparent activation energy (E_a) for the DDO path of 49.7 kJ mol^{-1}, significantly lower than that obtained on Pt(111) surfaces through theoretical calculations.[43,44] This relatively low activation energy could be a result of the participation of BAS in the Pt-catalyzed direct deoxygenation reaction, as suggested in previous work.[5] We also note that the data for the HYD path did not fit a single line. We used two segments and obtained an E_a value for when the temperature <290 °C of -4.2 kJ mol^{-1} and -69.7 kJ mol^{-1} for temperatures >290 °C. The negative E_a value clearly indicates that strongly exothermic elementary steps contribute to and dominate the hydrogenation of *m*-cresol[25,26,40–42] as well as the subsequent reaction steps.[25,26] The significant difference in the E_a value before and after 290 °C can be related to the contribution of the thermodynamic control to the overall reaction, which makes hydrogenation

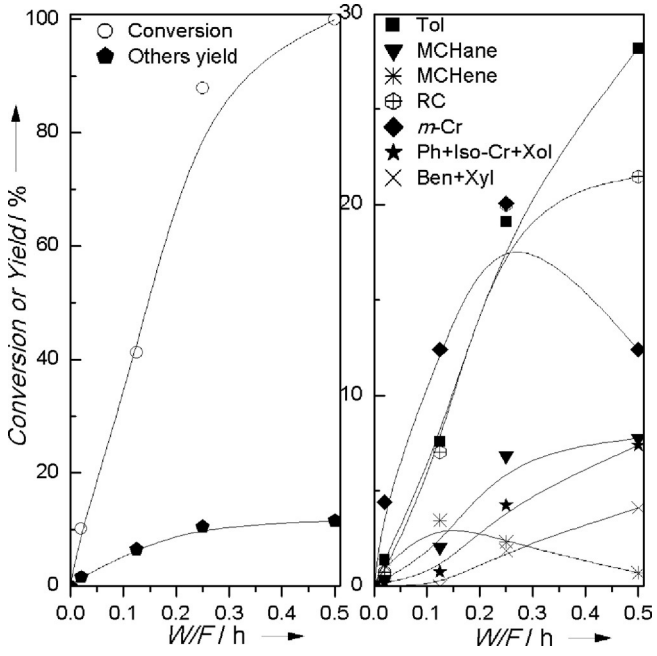

Figure 11. Effect of W/F on methylcyclohexanone (MCHone) conversion on Pt/HBeta at 350 °C. Reaction conditions: $T = 350$ °C, $P = 1$ atm, H_2/MCHone = 50, TOS = 0.5 h for each W/F.

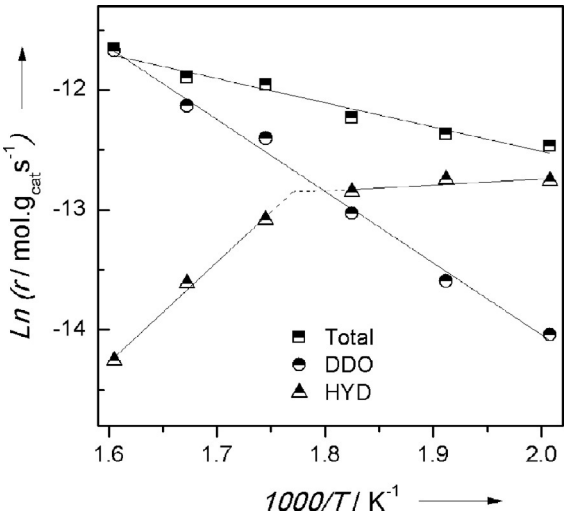

Figure 12. Arrhenius plots of *m*-cresol hydrodeoxygenation on Pt/HBeta at 225–350 °C. Reaction conditions: $P = 1$ atm, H_2/*m*-cresol = 50, TOS = 0.5 h for each data point, conversion is kept under 7% by adjusting the W/F value.

unfavorable at higher temperatures. Indeed, Shin and Keane showed that phenol is predominant over cyclohexanone and cyclohexanol in the thermodynamic equilibration on a Ni catalyst when temperature is increased to 300 °C.[40] Similarly, Pushkarev et al. also observed the Ln(turnover rate) [Ln(TOR)] values deviated from a linear regression line on the Arrhenius plot at higher temperatures during benzene hydrogenation on a Pt catalyst.[45] They attributed this behavior to the lowered surface coverage of hydrogen and reaction intermediates at higher temperatures as well as thermodynamic limits that make the forward exothermic hydrogenation unfavorable, particularly when the temperature is higher than 250 °C. The overall deoxygenation E_a is only 16.8 kJ mol^{-1}, possible owing to a combined contribution from the two reaction pathways.

Increasing reaction temperature would favor the endothermic reaction of the DDO path with a positive apparent activation energy. In contrast, the hydrogenation of *m*-cresol becomes unfavorable as it is an exothermic reaction with a negative activation energy for the overall HYD path, particularly at temperatures higher than 290 °C. In addition, increasing the temperature lowers the surface hydrogen coverage, and thus also hinders the initial hydrogenation of *m*-cresol. Therefore, the HYD path becomes less favorable whereas the DDO path becomes the major path as the temperature is increased.

There is a minimum at 275 °C in the conversion–temperature plot for the hydrodeoxygenation of *m*-cresol on Pt/SiO_2.[37] However, this was not observed on Pt/HBeta (Figure 10). It has been interpreted that the reduction in the hydrogenation rate of *m*-cresol cannot be compensated by the increase in the rates of deoxygenation of *m*-cresol on Pt/SiO_2 as the temperature is increased. The monotonic increase in *m*-cresol conversion on Pt/HBeta, therefore, could be a result of the increase in the direct deoxygenation rate being faster than the decrease in hydrogenation of *m*-cresol to MCHone and MCHol. The difference in the two catalysts indicates that the BAS participate in the Pt-catalyzed DDO of *m*-cresol, resulting in an enhanced reaction rate and compensating for the decrease due to the inhibition of the HYD path.

Comparison with literature results at high pressures

At 200–250 °C and 5 MPa hydrogen pressure using a metal/zeolite catalyst, the HYD path is the only reaction pathway in hydrodeoxygenation of phenolics, producing cyclohexanes as the major products.[13,14] This work showed that both the HYD and DDO paths are the major reaction pathways at the same reaction temperature, but at atmospheric hydrogen pressure. The different reaction pathways, and therefore the different product distributions, are clearly only related to the difference in the hydrogen pressures. Compared with direct deoxygenation, the hydrogenation reaction consumes 3 times more hydrogen. Increasing the hydrogen pressure would make the reaction more favorable toward hydrogenation than direct deoxygenation, as high pressure favors the molar reduction reaction. Furthermore, increasing the hydrogen pressure would increase the surface coverage of hydrogen on the Pt particles. Thus, the hydrogenation reaction is more favorable than direct deoxygenation. Because dehydration of MCHol on BAS is always faster than hydrogenation of *m*-cresol on Pt, once the initial reaction is shifted to hydrogenation, the reaction would eventually turn to the HYD path. The results of the present study indicate that temperature and pressure have a strong influence on the initial reaction (hydrogenation or direct deoxygenation) on Pt, and therefore determine the overall reaction path.

Ring contraction

The isomerization (including ring contraction) of alkanes on the Pt/zeolite bifunctional catalyst is generally believed to follow the carbenium ion mechanism: dehydrogenation of alkanes on Pt to olefins, the olefin is then protonated by adjacent BAS forming the carbenium ion, which is rearranged to another olefin through a cyclopropyl carbenium ion transition state followed by the olefin hydrogenation to alkane product.[46] McVicker et al. showed that MCHane ring contraction can be used as a probe reaction to characterize the acidity of Pt-loaded zeolites by analyzing the reaction rates and product distributions.[47] In the current work, the yield of ECP at low conversion of *m*-cresol is only slightly higher than the individual yield of DMCP isomers. ECP converts to DMCP at higher conversions at 250 °C, confirming the strong acidity of Pt/HBeta.

The formation rate of the RC products from MCHene is slightly faster than that from MCHane but significantly faster than from Tol (Figure 9). This trend is clearly related to the feasibility of formation of MCHene, which is readily protonated on BAS to form the carbenium ion for ring contraction. The fact that RC is favored over Tol when the HYD intermediates were fed into the reaction (Figures 7–9), but Tol is favored over the RC products when *m*-cresol is fed into the reaction (Figure 6), further supports that the formation of Tol is mainly through the DDO pathway. The higher RC yield is apparently related to the high yield of MCHene from dehydration of MCHol, which is readily ring contracted on BAS along the HYD path; whereas along the DDO path, the conversion rate of Tol to RC is slow owing to the undetectably low concentration of MCHene in the Tol hydrogenation (Figure 9C).

It is interesting to note that the 25% yield of the RC products at 250 °C is significantly higher than that observed in the liquid-phase reactions at high pressures (typically lower than 10%).[48] The RC yield can be further improved, approaching the thermodynamic limit of 50%, by increasing W/F (data not shown). If a selective ring-opening catalyst (such as Ir) is present, the RC products can be converted to branched alkanes with desirable octane numbers.[49] Note that the ring opening of cyclopentanes is much easier than that of cyclohexanes.[50] Therefore, the catalytic processes in the present study provide a straightforward approach to produce branched alkanes with desirable fuel properties under mild conditions. Moreover, the product distribution can be simply adjusted by controlling the reaction temperature. Relatively high temperatures (>350 °C) are suitable for aromatics when the aromatics are the desirable products and the hydrogen supply is limited. On the other hand, low reaction temperatures (<300 °C) are desirable when

the hydrogen supply is sufficient and the aromatics are undesirable. This is especially suited to current commercial applications as very low aromatic concentrations are allowed in fuel, whereas high octane numbers are required for fuel.

Conclusions

Hydrodeoxygenation of *m*-cresol at 250 °C under atmospheric hydrogen pressure produces toluene, methylcyclohexanone, and methylcyclohexane as the major products at low W/F values, but produces toluene, methylcyclohexane, and ring-contraction products (dimethylcyclopetanes and ethylcyclopentane) as major products at high W/F values. None of the possible intermediates (methylcyclohexanone, methylcyclohexanol, methylcyclohexene) of the HYD path produce a similar toluene yield as that of *m*-cresol either at low W/F values, when kinetics control the product distribution, or at high W/F values, when thermodynamic equilibria control the product distribution. These results indicate that two distinct major reaction pathways during *m*-cresol hydrodeoxygenation may operate: one is the direct deoxygenation (DDO) to toluene and the other is hydrogenation to methylcyclohexanol on Pt followed by dehydration to methylcyclohexene on the Brønsted acid sites (HYD) and further to the final products. Because the subsequent steps of dehydration of methylcyclohexanol and conversion of methylcyclohexene are significantly faster than those of Pt-catalyzed direct deoxygenation and hydrogenation of *m*-cresol, the rate-determining step of the HYD path is the initial hydrogenation of *m*-cresol. Consequently, which of the two pathways dominates the reaction depends on the balance between the initial direct deoxygenation and hydrogenation rate of *m*-cresol on Pt. Increasing the temperature improves the direct deoxygenation to toluene but inhibits the hydrogenation of *m*-cresol to methylcyclohexanol, resulting in DDO as the dominant path. The apparent activation energy of the direct deoxygenation path is 49.7 kJ mol^{-1} at 225–350 °C. The present study also showed that adjusting the reaction conditions provides a simple approach to control the formation of ring-contraction products and isoalkanes with desirable fuel properties under mild conditions.

Experimental Section

Catalyst preparation

The catalyst support of HBeta was obtained by calcination of the ammonium form of the Beta zeolite (Zeolyst, CP814C, Si/Al = 19, S_{BET} = 710 m^2 g^{-1}) at 550 °C for 6 h. Pt/HBeta (1 wt%) was prepared by incipient wetness impregnation of HBeta with an aqueous solution of $H_2PtCl_6{\cdot}6H_2O$ (Tianjin Kemiou Chemical) overnight. The resulting sample was then dried at 120 °C for 12 h, and calcined at 400 °C for 4 h.

Catalyst characterization

The bulk structure of the catalyst sample was characterized by powder X-ray diffraction (XRD) on a Rigaku D/max 2500 diffractometer. The Pt particle size distribution was evaluated by transmission electron microscopy (TEM) observation on a JEM 2010F system. The Pt dispersion was estimated by CO chemisorption in a microreactor system, equipped with gas delivery system and temperature control unit, and monitored by a Cirrus 200 mass spectrometer (MKS). The catalyst sample (50 mg, 40–60 mesh) was loaded into a quartz tube reactor (o.d. = 6 mm), reduced by flowing H_2 at 300 °C for 1 h, which was followed by He purging for 30 min at the same temperature to remove chemisorbed H_2 from the catalyst surface. Then, CO/He pulses (5%, 100 μL) were sent onto the catalyst by a six-port valve every 3 min after the temperature reached room temperature. The pulse was stopped when no more CO adsorption was observed. A CO/Pt stoichiometry of 1:1 was used to estimate the dispersion. The acid density was quantified by temperature-programmed desorption of NH_3 (NH_3-TPD) and isopropylamine (IPA-TPD) in the same system as the CO chemisorption. The sample pretreatment used the same procedure as the chemisorption. The adsorption, desorption, and quantification followed the procedure reported in previous work.[32]

Catalytic performance

Hydrodeoxygenation of *m*-cresol was investigated in a fixed-bed quartz tube (o.d. = 6 mm) reactor at atmospheric hydrogen pressure. The catalyst sample of 40–60 mesh was reduced in flowing H_2 at 300 °C for 1 h prior to the reaction, and then the temperature was adjusted to the reaction temperature. Gases were controlled by mass flow controllers, and *m*-cresol was fed into the reaction by using a syringe pump (Kd Scientific), and was vaporized before entering the reactor. All lines were heated to avoid any condensation of reactants and products. The products were quantified online in a gas chromatograph (GC 7890B, Agilent) equipped with an Innowax capillary column (60 m) and a flame ionization detector (FID). Product identification was performed with a GC-MS (Shimadzu QP2010SE), accompanied by standard sample injection. Space time (W/F, $g_{cat}\,g_{reactant}{}^{-1}\,h$) is defined as the ratio of catalyst mass (g) to organic feed flow rate (g h^{-1}). To follow the major products evolution, the W/F value was adjusted from 0 to 2 h by varying both the catalyst amount and organic feed flow rate. The H_2/organic feed molar ratio was kept at 50 in all runs. The conversion and yield are reported in mol_{carbon}%. To verify the major reaction path, the possible intermediates (3-methylcyclohexanone, 3-methylcyclohexanol, 4-methylcyclohexene, methylcyclohexane, and toluene) were also studied. The chemicals were purchased form Sigma–Aldrich and used without further purification, and the purity of the gases used was higher than 99.999%. The carbon mass balance was higher than 95% in all runs. Both qualitative and quantitative reproducibility have been tested for several selected operating conditions and the results showed that the relative uncertainties of conversion and selectivity are within ±2%.

Acknowledgements

The authors thank the support from the National Natural Science Foundation of China (21206116 and 21373148) and the Ministry of Education of China Program of New Century Excellent Talents in University (NCET-12-0407).

Keywords: hydrodeoxygenation · hydrogenation · *m*-cresol · Pt/HBeta · ring contraction

[1] A. J. Ragauskas, G. T. Beckham, M. J. Biddy, R. Chandra, F. Chen, M. F. Davis, B. H. Davison, R. A. Dixon, P. Gilna, M. Keller, P. Langan, A. K. Naskar, J. N. Saddler, T. J. Tschaplinski, G. A. Tuskan, C. E. Wyman, *Science* **2014**, *344*, 1246843.
[2] J. Zakzeski, P. C. A. Bruijnincx, A. L. Jongerius, B. M. Weckhuysen, *Chem. Rev.* **2010**, *110*, 3552 – 3599.
[3] C. Liu, H. Wang, A. M. Karim, J. Sun, Y. Wang, *Chem. Soc. Rev.* **2014**, *43*, 7594 – 7623.
[4] M. Saidi, F. Samimi, D. Karimipourfard, T. Nimmanwudipong, B. C. Gates, M. R. Rahimpour, *Energy Environ. Sci.* **2014**, *7*, 103 – 129.
[5] X. L. Zhu, L. L. Lobban, R. G. Mallinson, D. E. Resasco, *J. Catal.* **2011**, *281*, 21 – 29.
[6] G. T. Neumann, B. R. Pimentel, D. J. Rensel, J. C. Hicks, *Catal. Sci. Technol.* **2014**, *4*, 3953 – 3963.
[7] E. O. Odebunmi, D. F. Ollis, *J. Catal.* **1983**, *80*, 56 – 64.
[8] H. Weigold, *Fuel* **1982**, *61*, 1021 – 1026.
[9] E. Laurent, B. Delmon, *Ind. Eng. Chem. Res.* **1993**, *32*, 2516 – 2524.
[10] F. E. Massoth, P. Politzer, M. C. Concha, J. S. Murry, J. Jakowski, J. Simons, *J. Phys. Chem. B* **2006**, *110*, 14283 – 14291.
[11] Y. Romero, F. Richard, S. Brunet, *Appl. Catal. B* **2010**, *98*, 213 – 223.
[12] A. L. Jongerius, R. Jastrzebski, P. C. A. Bruijnincx, B. M. Weckhuysen, *J. Catal.* **2012**, *285*, 315 – 323.
[13] D. Y. Hong, S. J. Miller, P. K. Agrawal, C. W. Jones, *Chem. Commun.* **2010**, *46*, 1038 – 1040.
[14] C. Zhao, S. Kasokov, J. He, J. A. Lercher, *J. Catal.* **2012**, *296*, 12 – 23.
[15] T. Nimmanwudipong, R. C. Runnebaum, D. E. Blockab, B. C. Gates, *Energy Fuels* **2011**, *25*, 3417 – 3427.
[16] M. S. Zanuttini, B. O. D. Costa, C. A. Querini, M. A. Peralta, *Appl. Catal. A* **2014**, *482*, 352 – 361.
[17] W. Zhang, J. Chen, R. Liu, S. Wang, L. Chen, K. Li, *ACS Sus. Chem. Eng.* **2014**, *2*, 683 – 691.
[18] J. E. Peters, J. R. Carpenter, D. C. Dayton, *Energy Fuels* **2015**, *29*, 909 – 916.
[19] T. M. Huynh, U. Armbruster, M. Pohl, M. Schneider, J. Radnik, D. Hoang, B. M. Q. Phan, D. A. Nguyen, A. Martin, *ChemCatChem* **2014**, *6*, 1940 – 1951.
[20] L. Wang, J. Zhang, X. Yi, A. Zheng, F. Deng, C. Chen, Y. Ji, F. Liu, X. Meng, F. Xiao, *ACS Catal.* **2015**, *5*, 2727 – 2734.
[21] A. Ausavasukhi, Y. Huang, A. T. To, T. Sooknoi, D. E. Resasco, *J. Catal.* **2012**, *290*, 90 – 100.
[22] A. F. Foster, P. T. M. Do, R. F. Lobo, *Top. Catal.* **2012**, *55*, 118 – 128.
[23] X. L. Zhu, R. G. Mallinson, D. E. Resasco, *Appl. Catal. A* **2010**, *379*, 172 – 181.
[24] X. L. Zhu, L. L. Lobban, R. G. Mallinson, D. E. Resasco, *Energy Fuels* **2014**, *28*, 4104 – 4111.
[25] E. Shin, M. A. Keane, *Ind. Eng. Chem. Res.* **2000**, *39*, 883 – 892.
[26] E. Furimsky, *Appl. Catal. A* **2000**, *199*, 147 – 190.
[27] H. Ohta, B. Feng, H. Kobayashi, K. Hara, A. Fukuoka, *Catal. Today* **2014**, *234*, 139 – 144.
[28] S. Boonyasuwat, T. Omotoso, D. E. Resasco, S. P. Crossley, *Catal. Lett.* **2013**, *143*, 783 – 791.
[29] S. T. Oyama, T. Onkawa, A. Takagaki, R. Kikuchi, S. Hosokai, Y. Suzuki, K. K. Bando, *Top. Catal.* **2015**, *58*, 201 – 210.
[30] R. N. Olcese, M. Bettahar, D. Petitjean, B. Malaman, F. Giovanella, A. Dufour, *Appl. Catal. B* **2012**, *115 – 116*, 63 – 73.
[31] B. S. Gevert, J. E. Otterstedt, F. E. Massoth, *Appl. Catal.* **1987**, *31*, 119 – 131.
[32] X. L. Zhu, L. L. Lobban, R. G. Mallinson, D. E. Resasco, *J. Catal.* **2010**, *271*, 88 – 98.
[33] T. J. G. Kofke, R. J. Gorte, G. T. Kokotailo, W. E. Farneth, *J. Catal.* **1989**, *115*, 265 – 272.
[34] J. Huang, W. Long, P. K. Agrawal, C. W. Jones, *J. Phys. Chem. C* **2009**, *113*, 16702 – 16710.
[35] L. Brabec, J. Novakova, L. Kubelkova, *Stud. Surf. Sci. Catal.* **1994**, *84*, 1889 – 1896.
[36] S. C. Reyes, J. H. Sinfelt, G. J. DeMartin, *J. Phys. Chem. B* **2005**, *109*, 2421 – 2431.
[37] C. Chen, G. Chen, F. Yang, H. Wang, J. Han, Q. Ge, X. L. Zhu, *Chem. Eng. Sci.* **2015**, *135*, 145 – 154.
[38] L. Nie, D. E. Resasco, *J. Catal.* **2014**, *317*, 22 – 29.
[39] M. Dobrovolszky, Z. Tétényi, Z. Paál, *J. Catal.* **1982**, *74*, 31 – 43.
[40] E. Shin, M. A. Keane, *J. Catal.* **1998**, *173*, 450 – 459.
[41] Y. Yoon, R. Rousseau, R. S. Weber, D. Mei, J. A. Lercher, *J. Am. Chem. Soc.* **2014**, *136*, 10287 – 10298.
[42] G. Li, J. Han, H. Wang, X. L. Zhu, Q. Ge, *ACS Catal.* **2015**, *5*, 2009 – 2016.
[43] J. Lu, S. Behtash, O. Mamun, A. Heyden, *ACS Catal.* **2015**, *5*, 2423 – 2435.
[44] K. Lee, G. H. Gu, C. A. Mullen, A. A. Boateng, D. G. Vlachos, *ChemSusChem* **2015**, *8*, 315 – 322.
[45] V. V. Pushkarev, K. An, S. Alayoglu, S. K. Beaumont, G. A. Sormorjai, *J. Catal.* **2012**, *292*, 64 – 72.
[46] W. Knaeble, R. T. Carr, E. Iglesia, *J. Catal.* **2014**, *319*, 283 – 296.
[47] G. B. McVicker, O. C. Feeley, J. Z. Ziemiak, D. E. W. Vaughan, K. C. Strohmaier, W. R. Kliewer, D. P. Leta, *J. Phys. Chem. B* **2005**, *109*, 2222 – 2226.
[48] C. Zhao, J. He, A. A. Lemonidou, X. Li, J. A. Lercher, *J. Catal.* **2011**, *280*, 8 – 16.
[49] M. Santikunaporn, W. E. Alvarez, D. E. Resasco, *Appl. Catal. A* **2007**, *325*, 175 – 187.
[50] G. B. McVicker, M. Daage, M. S. Touvelle, C. W. Hudson, D. P. Klein, W. C. Baird, Jr., B. R. Cook, J. G. Chen, S. Hantzer, D. E. Vaughan, E. S. Ellis, O. C. Feeley, *J. Catal.* **2002**, *210*, 137 – 148.

Received: November 9, 2015
Published online on January 12, 2016